Molecular Genetics and Metabolism xxx (xxxx) xxx–xxx

Contents lists available at ScienceDirect

Molecular Genetics and Metabolism

journal homepage: www.elsevier.com/locate/ymgme

Regular Article

Dysregulated autophagy in restrictive cardiomyopathy due to Pro209Leu mutation in BAG3

A. Schänzer[a,*], S. Rupp[b], S. Gräf[a], D. Zengeler[c], C. Jux[b], H. Akintürk[b], L. Gulatz[a], N. Mazhari[b], T. Acker[a], R. Van Coster[d], B.K. Garvalov[a,e,1], A. Hahn[f,1]

[a] Institute of Neuropathology, Justus Liebig University Giessen, 35392 Giessen, Germany
[b] Pediatric Heart Center, Justus Liebig University Giessen, 35392 Giessen, Germany
[c] Center for Genomics and Transcriptomics (CeGat) GmbH, 72076 Tübingen, Germany
[d] Division of Child Neurology, Department of Pediatrics, University Hospital Gent, 9000 Gent, Belgium
[e] Department of Microvascular Biology and Pathobiology, Centre for Biomedicine and Medical Technology Mannheim (CBTM), Medical Faculty Mannheim, University of Heidelberg, 68167 Mannheim, Germany
[f] Department of Child Neurology, Justus Liebig University Giessen, 35392 Giessen, Germany

ARTICLE INFO

Keywords:
Myopathy
Restrictive cardiomyopathy
BAG3
Autophagy
Mitophagy
Myofibrillar myopathy
MFM
OXPHOS

ABSTRACT

Myofibrillary myopathies (MFM) are hereditary myopathies histologically characterized by degeneration of myofibrils and aggregation of proteins in striated muscle. Cardiomyopathy is common in MFM but the pathophysiological mechanisms are not well understood. The BAG3-Pro209Leu mutation is associated with early onset MFM and severe restrictive cardiomyopathy (RCM), often necessitating heart transplantation during childhood. We report on a young male patient with a BAG3-Pro209Leu mutation who underwent heart transplantation at eight years of age. Detailed morphological analyses of the explanted heart tissue showed intracytoplasmic inclusions, aggregation of BAG3 and desmin, disintegration of myofibers and Z-disk alterations. The presence of undegraded autophagosomes, seen by electron microscopy, as well as increased levels of p62, LC3-I and WIPI1, detected by immunohistochemistry and western blot analyses, indicated a dysregulation of autophagy. Parkin and PINK1, proteins involved in mitophagy, were slightly increased whereas mitochondrial OXPHOS activities were not altered. These findings indicate that altered autophagy plays a role in the pathogenesis and rapid progression of RCM in MFM caused by the BAG3-Pro209Leu mutation, which could have implications for future therapeutic strategies.

1. Introduction

Myofibrillar myopathies (MFM) are a group of progressive hereditary neuromuscular disorders, which typically have a late onset and are frequently associated with cardiac involvement [1]. Pathogenic mutations in several different genes were found to be associated with MFM, including *DES* (desmin), *CRYAB* (αB-crystallin, also known as HSPB5, heat shock family B member 5), *MYOT* (myotilin), *LDB3* (LIM domain binding 3, also known as *ZASP*, Z-band alternatively spliced PDZ containing protein), *FLNC* (filamin C), *FHL1* (four and a half LIM domains 1), *TTN* (titin), and *BAG3* (bcl-2 associated athanogene 3). These proteins are located at the Z-disks and pathogenic mutations affecting them can result in protein aggregation and disintegration of myofibrillar architecture [2–10]. In some instances, the protein aggregates show specific morphologic characteristics indicative of the underlying mutation [11].

Mutations in *BAG3* are a rare cause of MFM. A proline to leucine mutation in the second IPV domain of BAG3 (BAG3-Pro209Leu) is associated with rapidly progressive restrictive cardiomyopathy (RCM), often requiring heart transplantation during childhood. Additional symptoms such as proximal myopathy, neuropathy, rigid spine and ventilatory insufficiency may precede or succeed the clinical signs of RCM [12–17] (Table 1). In some patients with Pro209Leu mutation, light microscopic examination showed intracytoplasmatic inclusions in skeletal muscle containing the Z-disk proteins desmin and αB-crystallin, and electron microscopic examination revealed disintegration and disarray of myofibrils with aggregates of degraded filaments and electron dense material [13,14,16].

Autophagy in striated muscle is a complex process that involves different pathways and is crucial for protein homeostasis during

* Corresponding author at: Institute of Neuropathology, Justus Liebig University Giessen, Arndtstrasse 16, 35392 Giessen, Germany.
E-mail address: anne.schaenzer@patho.med.uni-giessen.de (A. Schänzer).
[1] Contributed equally to the manuscript.

https://doi.org/10.1016/j.ymgme.2018.01.001
Received 25 September 2017; Received in revised form 2 January 2018; Accepted 2 January 2018

Table 1
Clinical and morphological findings in patients with myofibrillar myopathy and Pro209Leu mutation in the BAG3gene.

Reference	Mutation	Age of onset (y) and sex	Cardiomyopathy	Myopathy	Neuropathy	Rigid spine	Respiratory failure	Morphology
Lee et al. [16]	Pro209Leu c.626C > T and germline variation c.772C > T	6 (F)	RCM	+	+	+	+	Muscle biopsy: electron dense granulofilamentous material, minicores Nerve biopsy: axonopathy
Konersman et al. [12]	Pro209Leu c.626C > T	8 (M)	RCM (HTX at 8y)		+		+	Muscle biopsy: neurogenic and myopathic changes; scattered fibers with inclusions and vacuoles Heart explant: cytoplasmic inclusions Nerve biopsy: nearly complete loss of larger myelinated fibers
Selcen et al. [13]	Pro209Leu c.626C > T	10 (M) 14 (F) 11 (M)	RCM (HTX at 13y) HCM RCM	+ + +		 + +	+ + +	Muscle biopsy: protein accumulation, Z disk streaming and accumulation of electron dense structures, disarray of myofibrils, mitochondrial cluster and apoptotic nuclei
Odgerel et al. [14]	Pro209Leu	9 (M) 12 (M) 12 (F) 5 (M)	RCM (died at 9y) RCM (HTX at 14y) RCM (died at 20y) RCM at 10y (HTX at 13y, died at 15y)	+ + + +	+ 	 	+ + + +	Muscle biopsy: desmin positive inclusions, myofibrillar breakdown, Z –line streaming, electron dense filamentous and granular material disrupting the Z-lines Nerve biopsy: reduction of myelinated fibers with giant axons
Kostera-Pruszczyk et al. [15]	Pro209Leu c.626C > T	12 (F)	Asymptomatic long QT syndrome	+	+			Muscle biopsy: core like structure
Jaffer et al. [17]	Pro209Leu c.626C > T	13 (F) 8 (M) 14 (F)	RCM (HTX) RCM RCM	+ + (+)		+ (+)	 +	Muscle biopsy: accumulation of desmin and myotillin, granulomatous material, myofibrillar loss, Z-line streaming Nerve biopsy: giant axons
Noury et al. [40]	Pro209Leu c.626C > T	24 (F)	No	+	+	+		Muscle biopsy: accumulation of granulofilamentous material originating from the Z-disk disrupting the sarcomeres and in subsarcolemmal areas, dense granulomatous material

HCM = Hypertrophic Cardiomyopathy; HTX = heart transplantation; RCM = restrictive cardiomyopathy; y = years; M = Male; F = Female.

tension-induced stress [22–24]. The autophagy cascade can be upregulated due to various forms of cellular stress and is dysregulated in different diseases [20,25,26]. BAG3 plays a key role in selective macroautophagy. Although expressed in various tissues, BAG3 is particularly abundant in mechanically strained skeletal and cardiac muscle cells [18]. It is necessary for the Z-disk integrity and is important for autophagy of damaged or misfolded protein in striated myocytes [19–21]. BAG3 is upregulated under mechanical stress and induces the formation of a multicomponent heat shock machinery at the Z-disk involving heat shock protein (Hsp70) and small heat shock proteins (HSPBs), necessary for delivery of targeted proteins to autophagosomes [27–35]. In addition, BAG3 regulates local mTORC1 function and is involved in filamin protein synthesis [22,36]. In the heart, it protects cardiomyocytes against proteotoxic stress and mutation in the *BAG3* gene has been associated with sarcomere disarray and reduced contraction power in cardiomyocytes, as well as with dilated cardiomyopathy [21,37].

Taking into account the multiple functions of BAG3 in controlling protein homeostasis and autophagy in striated muscle, a mutation in the gene may result in a defect of myocyte function. In line with this notion, *Bag3*-deficient mice develop fulminant myofibrillar myopathy with early lethality [18,38]. In zebrafish, overexpression of the mutant BAG3-Pro209Leu results in aggregate formation, while loss of wild type BAG3 causes myofibrillar disintegration [39].

In contrast to skeletal muscle, morphologic alterations in cardiac tissue have not been analyzed in detail [12], thereby limiting the pathophysiological understanding of the BAG3-Pro209Leu-related RCM and impeding the development of new therapeutic strategies. Here, we performed comprehensive morphological and biochemical analyses in explanted heart tissue from a patient with RCM caused by the BAG3-Pro209Leu mutation, focusing on the assessment of protein aggregation, myofibrillar structure and autophagy.

2. Methods

2.1. Cardiac muscle analysis

This work was approved by the Ethics Committee of the University of Giessen and a written informed consent was obtained from all parents. Tissue samples from the patient's explanted heart (P) and from two controls were analyzed. One control tissue was from an eight-year-old child with pulmonary atresia with intact ventricular septum (intraoperative biopsy) (C1), and one was an explanted heart from a one-year-old child with hypoplastic left heart syndrome (C2).

2.2. Next generation sequencing

To identify the causative gene, next-generation sequencing of genes in which pathogenic variants had previously been associated with neuromuscular diseases (in total 483 genes, 1370 kb) was performed. The panel for congenital and distal myopathies was analyzed in detail, due to the patient's clinical diagnosis. Details of panel design, library preparation, capture sequencing and variant calling have been published previously [41].

2.3. Histochemical, immunohistochemical and immunofluorescence microscopy

Unfixed heart tissue was snap frozen and 6 µm cryosections were stained with hematoxylin and eosin (HE), cytochrome oxidase (COX) and succinate dehydrogenase (SDH), according to standard procedures for analyzing skeletal muscle biopsies. From formalin fixed tissue, 3 µm sections were stained with H&E, Masson trichrome and congo red. Immunohistochemical analysis was performed on cryosections and paraffin sections using a Bench Mark XT automatic staining platform (Ventana, Heidelberg, Germany) with the following primary antibodies: mouse monoclonal anti-desmin (M076029-2, Agilent, 1:1000, Santa Clara, US); mouse monoclonal anti-LC3 (0231-100/LC3-5F10, nanoTools, 1:100, Teningen, Germany); mouse monoclonal anti-p62 (610832, BD Biosciences, 1:500, Franklin Lakes, US); mouse monoclonal anti-αB-crystallin (MONX10736, Monosan, 1:75, Uden, The Netherlands); rabbit polyclonal anti-ubiquitin (Z0458, DAKO, 1:300, Glostrup, Denmark). The following primary antibodies were used for immunofluorescence staining: mouse monoclonal anti-desmin (M076029-2, Agilent, 1:100, Santa Clara, US); rabbit polyclonal anti-BAG3 (10599-1-AP, Proteintech, 1:500, Manchester, UK). The secondary antibodies were: Alexa Fluor 568 goat anti-rabbit IgG (Life Technologies, 1:100, Carlsbad, US) and Alexa Flour 488 goat anti-mouse (Life Technologies, 1:500, Carlsbad, US). The sections were mounted with Fluoroshield mounting medium with DAPI (Abcam) and examined using a Nikon Eclipse 80i or Leica DM2000 fluorescence microscopes.

2.4. Transmission electron microscopy (TEM)

Small biopsies were fixed with 6% glutaraldehyde/0.4 M phosphate buffered saline (PBS) and were processed with a Leica EM TP tissue processor. For electron microscopy, ultrathin sections were contrasted with 3% lead citrate trihydrate with a Leica EM AC20 (Ultrastain kit II) and were examined using a Zeiss EM 109 transmission electron microscope.

2.5. Determination of protein expression in heart tissue

Unfixed heart tissue samples were lysed in 10 mM Tris HCl pH 7.5, 2% SDS, 2 mM EGTA, 20 mM NaF and homogenized using a mechanical homogenizer (T10 Ultra-Turrax, IKA, Staufen, Germany) and an ultrasound sonifier (Sonopuls Bandelin, Berlin, Germany). Protein concentration was determined using the DC protein assay (Bio-Rad, Munich, Germany). Equal amounts of total protein (30 µg of each sample) were loaded on an SDS-PAGE gel, transferred to a PVDF-membrane (Thermo Fisher Scientific, Dreieich, Germany, #88518) and analyzed using the following primary antibodies: rabbit polyclonal anti-BAG3 (10599-1-AP, Proteintech, 1:100.000, Manchester, UK); mouse monoclonal anti-desmin (M076029-2, Agilent, 1:1000, Santa Clara, US); mouse monoclonal anti-p62 (610832, BD Biosciences, 1:500, Franklin Lakes, US); mouse monoclonal anti-LC3 (0231-100/LC3-5F10, nanoTools, 1:1:1000, Teningen, Germany); mouse monoclonal anti-WIPI (ST1505, Merck Millipore, 1:500); rabbit polyclonal anti-ubiquitin (Z0458, DAKO, 1:1000, Glostrup, Denmark); mouse monoclonal anti-HSP70 (ADI-SPA-810-D, Enzo Life Science, 1:1000 Farmingdale, New York), mouse anti-αB-crystallin (HSPB5, MONX10736, Monosan, 1:250, Uden, The Netherlands); rabbit monoclonal anti-HSP6 (HSP20, ab184161, Abcam, 1:10,000, Cambridge, UK), rabbit monoclonal anti-HSP7 (cvHSP, ab150390, Abcam, 1:5000, Cambridge, UK), rabbit polyclonal anti-HSPB8 (HSP22, ab96837, Abcam, 1:1000, Cambridge, UK), rabbit polyclonal anti-parkin (ab15954, Abcam, 1:10.000, Cambridge, UK); rabbit monoclonal anti-PINK1 (6946T, Cell Signaling Technology, 1:500, Danvers, USA), mouse monoclonal anti-TOMM20 (ab56783, Abcam, 1:500, Cambridge, UK); rabbit monoclonal anti-BNIP3L (NIX, 12396S, Cell Signaling Technology, 1:500, Danvers, USA); rabbit polyclonal anti-pan-actin (4968, Cell Signaling, 1:1000, Danvers, US). Protein amounts were quantified by densitometric measurement of integrated band intensities using ImageJ/Fiji [42] and normalized to the levels of the house-keeping gene (pan-actin).

2.6. Quantitative reverse transcription (RT)-PCR

The tissue was lysed using a mechanical homogenizer (Precellys 24, Bertin Technologies, Rockville, US), RNA was isolated with an RNeasy Mini Kit (Qiagen, Hilden, Germany #74106) and reverse transcribed using iScript cDNA Synthesis kit (Biorad, Germany, #170–8891). cDNA

was amplified using the ABsolute QPCR SYBR Green Mix (Thermo Fisher Scientific, Dreieich, Germany, #AB1162/b) and a StepOnePlus real-time PCR system (Applied Biosystems). The primers used for BAG3 quantification were: hBAG3 For: CCCCGTTCAGGTCATCTGTC and hBAG3 Rev: AGGTGCAGTTTCTCGATGGG. The difference in the threshold number of cycles between the gene of interest and hypoxanthine phosphoribosyltransferase 1 (HPRT), used a "house-keeping" gene and amplified with primers HPRT1 For: TATGGCGACCCGCAG CCC and HPRT1 Rev: GCAAGACGTTCAGTCCTGTCCAT, was normalized relative to the standard chosen for the experiment and converted into x-fold difference.

2.7. Analysis of mitochondrial enzyme activities

The activities of citrate synthase and the complexes I (NADH-CoQ reductase), II (succinate CoQ oxidoreductase), II + III (succinate cytochrome *c* reductase) and IV (cytochrome *c* oxidase) were measured by spectrophotometric analysis as described previously [43–45]. The enzyme activities in the patient and two controls were analyzed in the same run. The enzyme activities in the patient were compared with the activities in two controls and with historical control data (n = 22). Enzyme activities are expressed as nmol/min/mg protein. For enzyme ratios the Z-score in brackets is calculated from the logarithm of OXPHOS activity divided by the logarithm of citrate synthase activity. Values lower than − 1.96 are significantly different ($P < 0.05$) from control samples and indicate deficient activities. Control sample ratios are given as mean ± SD.

3. Results

3.1. Case history

The patient is the second child born to healthy non-consanguineous German parents. At age four years, a heart murmur was noticed. A subsequent echocardiogram was suggestive of restrictive cardiomyopathy, later confirmed by MRI (Fig. 1) and endomyocardial biopsy. The patient's cardiac function remained stable until age six years, when he started complaining about dyspnea during minor exertion. In addition, nocturnal hypoxemia and hypercapnia were detected, necessitating non-invasive assisted ventilation overnight. The patient's cardiac function further deteriorated, ultimately leading to heart transplantation at age 8½ years.

Since the patient's physical endurance did not improve as expected and nocturnal hypoventilation persisted, a detailed neurological examination was performed at age nine years, revealing mild scoliosis and proximal muscle weakness. Serum creatinine kinase (CK) values were slightly increased (227 U/l; normal < 180 U/l). His vital capacity was substantially reduced (850 ml; 53% of the expected normal value). Electromyography of the right deltoid muscle disclosed a myopathic pattern, while electroneurography demonstrated a combined demyelinating and axonal polyneuropathy.

As the patient had a combination of RCM, skeletal myopathy and polyneuropathy, next generation sequencing was performed, targeting genes associated with cardiomyopathy and skeletal myopathy, which revealed a heterozygous Pro209Leu mutation in BAG3 [39]. Both parents did not carry the mutation.

3.2. The pathology of BAG3-Pro209Leu mutant cardiac tissue is characterized by abundant intracytoplasmic inclusions and myofibrillar disintegration with Z-disk alterations

Histological and histochemical analyses of BAG3-mutant cardiac tissue (Fig. 2 E-L) compared to cardiac tissue from control 1 (Fig. 2A-D) showed variation of cardiomyocyte diameter, hyperchromatic nuclei and focal fibrosis, which are morphological findings consistent with hypertrophic cardiomyopathy in the patient (Fig. 2E, F). Intracytoplasmic inclusions were abundant and strongly visible in many fibers with different staining (H&E, Masson trichrome, Gomori Trichrome, Congo red, Fig. 2E, F, J). Using enzymatic stains (SDH), the inclusions were presented as empty spaces similar to hyaline bodies, while the blue-stained myofibrils were displaced to the borders, suggesting myofibrillar disintegration (Fig. 2G). COX negative fibers were not visible (data not shown). Immunohistochemical staining disclosed that the intracytoplasmic inclusions contained different proteins such as

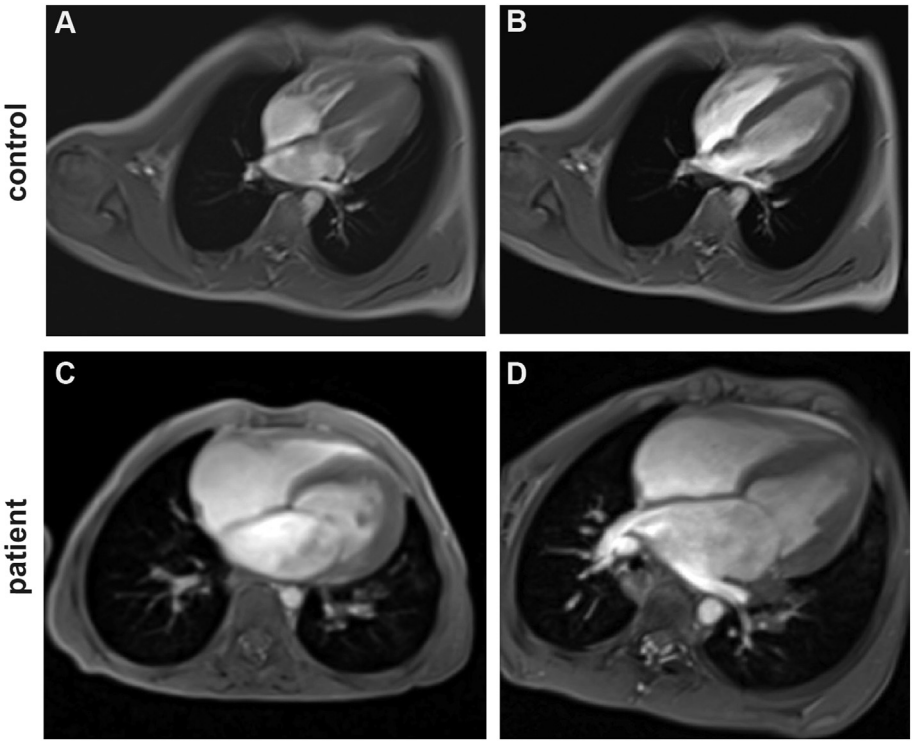

Fig. 1. Cardiac MR images of a ten-year-old control (A, B) and the patient (C, D) before transplantation during systole (A, C) and diastole (B, D). Four chamber views depict only minimal changes of the right and left chamber diameter from systole to diastole, distinctly enlarged atria, and moderate left ventricular wall thickening in the patient, consistent with a restrictive hypertrophic cardiomyopathy.

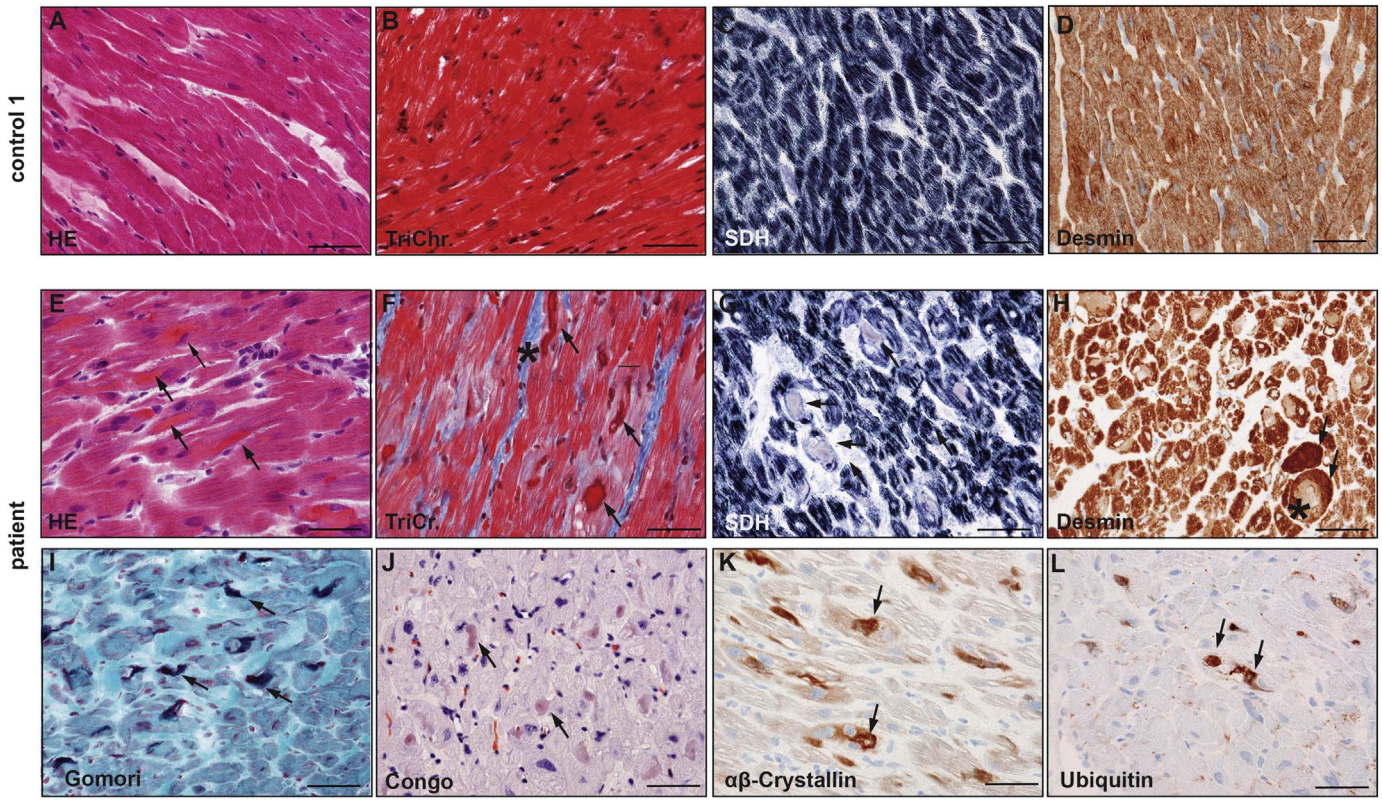

Fig. 2. Histological analyses of the patient's explanted heart (E-L) compared to control tissue (A–D). The patient's cardiac tissue reveals increased variability of fiber diameter with hyperchromatic nuclei (E) and endomyocardial fibrosis (*) (F). Many fibers contain intracytoplasmic inclusions (arrows), which are eosinophilic in H&E (E) and in Masson trichrome (F), dark in Gomori trichrome (I) and congophilic (J). Cryosections stained with SDH show large pale intracytoplasmic inclusions surrounded by focally displaced dark blue myofibrils (G). Immunohistochemical analyses demonstrate desmin positive (arrow) and desmin negative inclusions (*) (H) and accumulation of various proteins, including αB-crystallin (K) and ubiquitin (L). (Frozen sections: A, C, G, H; paraffin sections: B, D, F, J, H). Scale bars: 50 μm. (For interpretation of the references to colour in this figure legend, the reader is referred to the web version of this article.)

desmin, ubiquitin and αB-crystallin (Fig. 2H, K, L).

Ultrastructural findings in control and patient tissue are shown in Fig. 3. In the patient, strong myofibrillar disintegration and Z-disk alteration are visible (Fig. 3D). Disrupted Z-disks with Z-disk streaming and electron dense thick bundles, apparently originating from the Z-disks, were present in many fibers (Fig. 3E). Additional thick electron dense filamentous bundles were observed, partly surrounded by empty vacuoles, and vacuoles containing “myelin bodies” (Fig. 3G, H) and masses of partly subsarcolemmally located granulo-filamentous material (data not shown). Empty vacuoles and vacuoles filled with glycogen or electron dense material were frequent in the patient's cardiomyocytes (Fig. 3D, G–I), but not in control tissue (Fig. 3A). In the patient, the mitochondria showed mild abnormalities such as focal aggregation, polymorphic shape, and some focal lipofuscin droplets (Fig. 3F).

3.3. Altered expression of desmin and BAG3 in cardiac muscle of the patient with BAG3-Pro209Leu mutation

To assess the levels of BAG3 and desmin in BAG3-mutant cardiac tissue, we performed western blot analysis. This showed slightly increased desmin levels as compared to control samples (Fig. 4A, B), consistent with the large number of desmin positive aggregates detected by immunohistochemistry and immunofluorescence analysis (Fig. 2H). BAG3 protein levels in BAG3-mutant cardiomyocytes were similar or slightly higher than those in the control samples (Fig. 4A, B). The level of BAG3 mRNA was not increased (Fig. 4C). Further immunofluorescence studies revealed that both desmin and BAG3 were strongly expressed at Z-disks and intercalated disks in control cardiomyocytes (C1) (Fig. 4D–I). By contrast, both proteins were focally diminished at Z-disks in BAG3-mutant cardiac tissue, but strongly enriched in aggregates (Fig.4J–O). While some of the abundant protein aggregates contained either desmin or BAG3 (Fig. 4J–O), others showed co-localization of desmin and BAG3 (Fig. 4L, O).

3.4. Impaired autophagy in BAG3-Pro209Leu mutant cardiac muscle

Since BAG3 has been shown to be involved in autophagy, we tested whether this process is altered in BAG3-mutant cardiac tissue. Immunohistochemical staining showed many p62- and LC3-positive inclusions in the patient's cardiomyocytes (Fig. 5C, F). Electron microscopic examination showed vacuoles delimited by a double membrane separated by a cleft as characteristic of undegraded autophagosomes, containing cellular debris [46] (Fig. 5I). No such vacuoles were observed in the control samples (Fig. 5G, H).

We next examined by western blot the total levels of p62 and LC3, as well as of WD repeat domain phosphoinositide-interacting protein 1 (WIPI1), a marker of nascent autophagosomes. This revealed greatly increased expressions of p62, LC3-I, and WIPI1, but not of LC3-II in the cardiac tissue of the BAG3-Pro209Leu mutant tissue compared to the control samples (Fig. 6A, B). Furthermore, total levels of ubiquitinated proteins were considerably higher in the patient than in the controls.

BAG3 associates with heat shock protein 70 (HSP70), acting as a co-chaperone, and has also been shown to bind members of the small heat shock protein family (HSPBs [47,48]). Moreover, a complex of BAG3 with HSP70 and/or HSPB8 was reported to play a role in the selective degradation of misfolded or damaged proteins by macroautophagy [20,21,27–29]. Therefore, we assessed the levels of these heat shock proteins. While there was no change in HSP70 expression, we observed increased levels of all members of the small HSPs, especially HSPB6, in the patient (Fig. 6C, D).

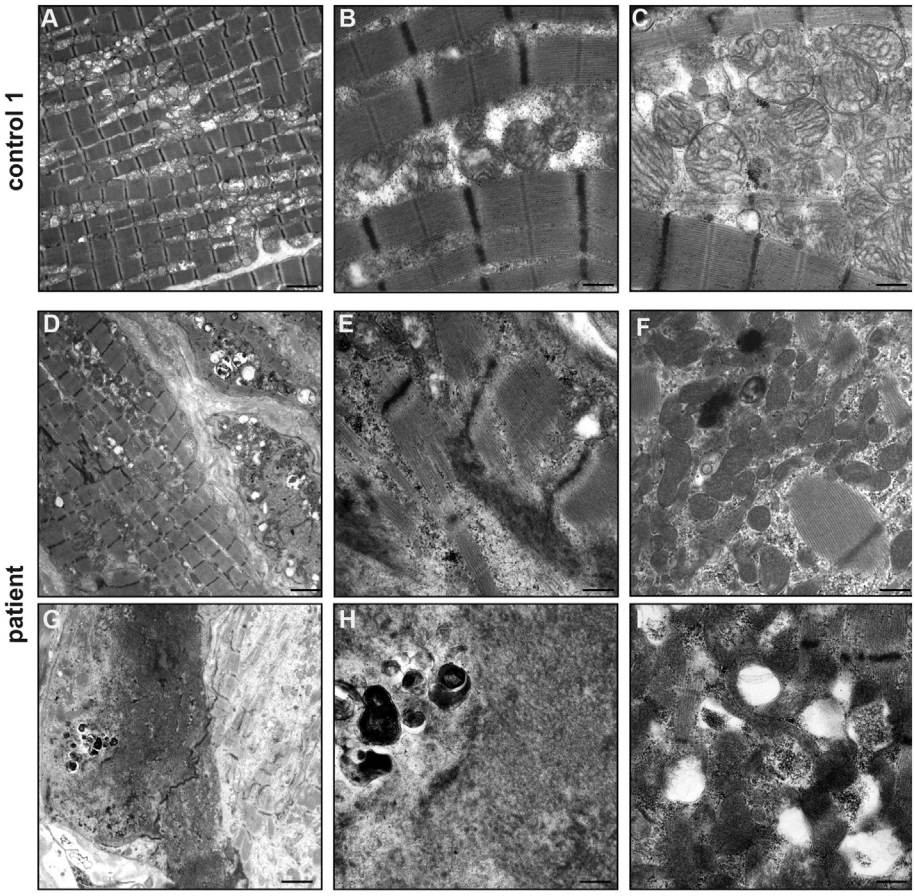

Fig. 3. Ultrastructural findings in control 1 (A–C) and BAG3-mutant cardiac tissue (D-I). In BAG3-mutant tissue, the cardiomyocytes show severe myofibrillar disintegration with strong variation of diameter and atrophic cells with vacuoles (D). Z-disk alterations are frequent and electron dense material originating from the Z-disks is abundant (E). Focal accumulation of mitochondria with some lipofuscin droplets are also visible (F). Electron dense thick bundles, partly surrounded by vacuoles containing electron dense material, are frequent (G, H). In addition, empty vacuoles and vacuoles filled with glycogen or electron dense material are located between myofibrillar bundles (I). Scale bars: A, D, G: 2.5 µm; B, C, E, F, H, I: 0.5 µm.

3.5. Normal mitochondrial enzyme activities but potential alteration of mitophagy in BAG3-Pro209Leu mutant cardiac muscle

As alterations of mitochondrial function have been described previously in skeletal muscle biopsies from patients with MFM [49–51], we investigated mitochondrial function and mitophagy in BAG3 mutant cardiac tissue using histological, ultrastructural, western blotting and biochemical analyses. In the patient's heart tissue, COX-negative fibers were not detected (data not shown). Spectrophotometric measurements of oxidative phosphorylation (OXPHOS) enzyme activities did not reveal significant differences between the patient, two control samples (C1, C2) and historical controls (n = 22) (Table 2). With TEM, many BAG3-mutant cardiomyocytes showed some focal accumulations of mitochondria with moderate polymorphic appearance (Fig. 3F).

Mitochondria can undergo morphological and functional alterations even under physiological conditions. Degrading these altered mitochondria through a form of autophagy termed mitophagy is an important step in cellular homeostasis [52]. One of the possible functions of BAG3 is to promote mitophagy, as reduction of functional BAG3 protein was shown to be associated with impaired clearance of damaged mitochondria [53]. Using western blot analysis, we tested the abundance of Parkinson's disease (PD) associated proteins parkin and PTEN-induced putative kinase 1 (PINK1), key components of mitochondrial quality control [54–56], and of BCL2 interacting protein 3 like (BNIP3L)/NIX, a regulator of nonselective mitophagy during hypoxia [57,58]. In addition, we analyzed the mitochondrial import receptor subunit TOMM20, as a marker for mitochondrial load.

We found a slight increase in the levels of parkin and PINK1 in BAG3-mutant cardiac tissue compared to control samples, whereas BNIPlL/NIX was slightly decreased (Fig. 7A, B). The levels of TOMM20 were also slightly lower in patient tissue, suggesting that there was no increase in mitochondrial load (Fig. 7A, B). These data are in line with the normal activity of citrate synthase found in the patient's cardiac muscle (Table 2). Immunofluorescence staining with antibodies against SOD2 showed an irregular distribution of the mitochondria in the patient's cardiomyocytes (data not shown).

4. Discussion

Myofibrillar myopathies (MFM) are a subgroup of progressive neuromuscular disorders characterized morphologically by typical intracytoplasmic inclusions, containing proteins associated with myofibril disintegration, and by Z-disk alterations [2,4,7,9,59]. Similar morphological features have been described in patients with MFM caused by the BAG3-Pro209Leu mutation. However, the clinical symptoms in the latter differ from those seen in other forms of MFM, as the BAG3-Pro209Leu-related MFM usually has an early onset and can be associated with severe cardiomyopathy [12–17] (Table 1). Clinical findings such as proximal myopathy, polyneuropathy, rigid spine, early respiratory failure, and restrictive cardiomyopathy as the predominant clinical feature in our patient with BAG3-Pro209Leu mutation were consistent with those described in the literature for other individuals harboring this specific genetic defect. We performed a detailed morphological and biochemical analysis of the patient's explanted heart in an attempt to better understand the pathogenic mechanism leading to his cardiomyopathy. Our findings suggest that autophagic dysfunction may play a role in the pathogenesis and rapid progression of MFM associated with the BAG3-Pro209Leu mutation.

BAG3 has multiple functions in health and disease. It is expressed particularly abundantly in skeletal and cardiac muscle tissues, and is upregulated under mechanical stress [20,21,24,26,29–32]. We found that BAG3 was localized at the Z-disks and intercalated disks together with desmin in control cardiac tissue, consistent with the assumed role of BAG3 in maintaining Z-disk integrity. By contrast, both BAG3 and

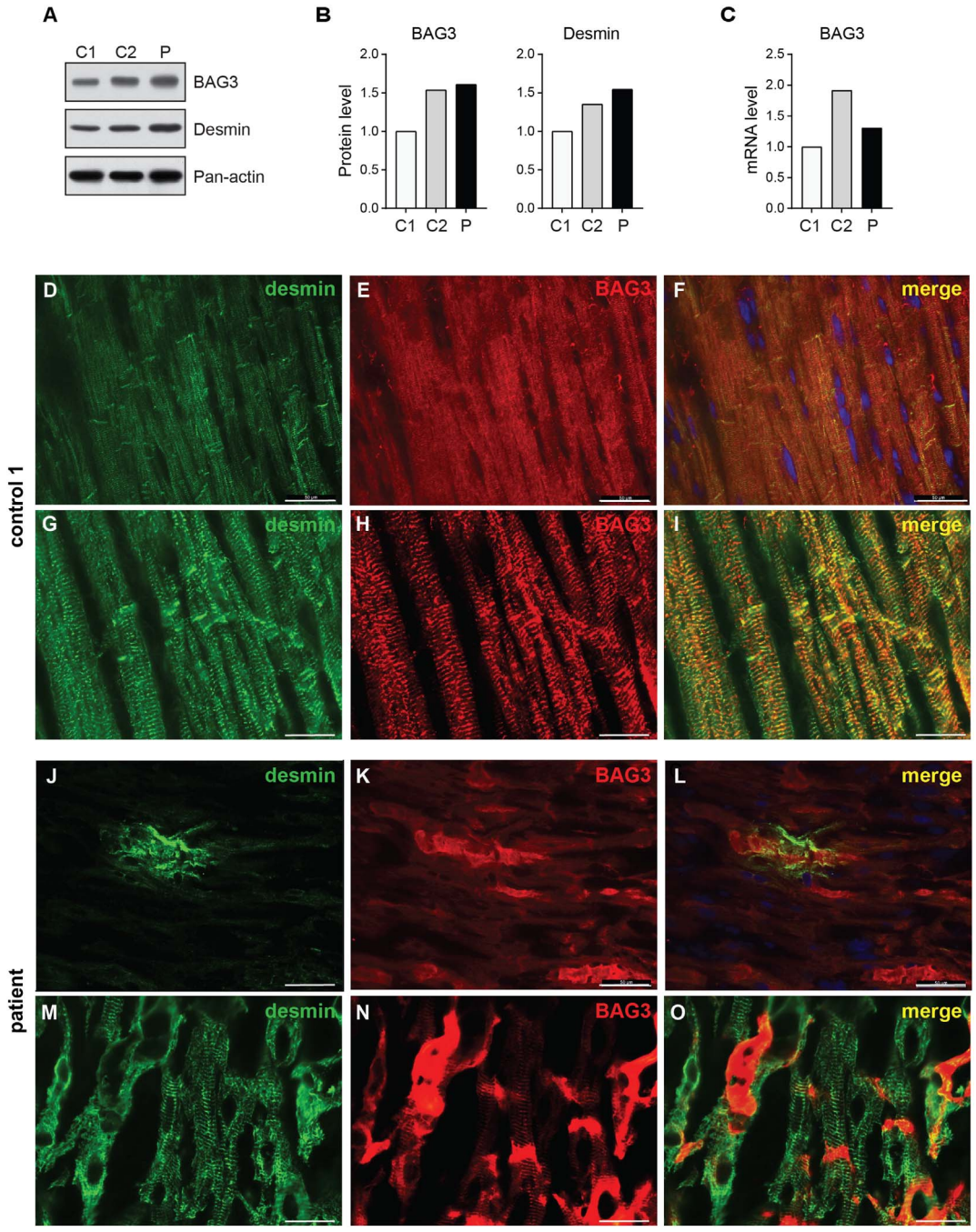

Fig. 4. Assessment of desmin and BAG3 levels, and localization of these proteins in cardiac tissue. A, B, western blot analysis of BAG3 and desmin levels in cardiac tissue from the controls C1 and C2, and from the BAG3-Pro209Leu mutant patient (P). Equal amounts of total protein were loaded and probed with the indicated antibodies; pan-actin served as a loading control (A). The amount of signal was densitometrically quantified and normalized to the level of pan-actin (B). BAG3 mRNA expression was determined using quantitative RT-PCR and normalized to the expression level of C1 (C). Immunofluorescence staining shows localization of desmin and BAG3 at the Z-disks and intercalated discs in healthy cardiomyocytes (D–I), whereas desmin and BAG3 are focally diminished at Z-disks and enriched in aggregates in cardiac tissue from the patient (J–O). BAG3 positive aggregates are frequent in the patient and are focally surrounded by desmin (J–O). Scale bars: D–F, J–L, 50 μm, G–I, M–O, 20 μm.

desmin expression was diminished in the Z-disks of the patient's cardiac muscle. This was accompanied by Z-disk disruption at the ultrastructural level, severe damage of myofibrillar architecture, and high variation of muscle fiber diameter, compatible with a severe form of cardiomyopathy. These findings are in line with histological abnormalities seen in skeletal muscle biopsies from other patients with various forms of MFM, including subjects harboring the BAG3-Pro209Leu mutation [2–4,11,14].

The morphological findings in our patient also match results from *in vitro* studies and *in vivo* experiments in animal models with loss of BAG3 function [21,31,38,39]. In particular, our findings are in perfect congruence with the presence of protein aggregates at the end stage of disease in *Bag3*-deficient mice, which develop a fulminant myofibrillar myopathy [18].

The underlying etiopathogenic mechanisms of MFM are still not sufficiently understood. Recent findings suggest that the accumulation of protein aggregates is not due to increased protein production, but is rather caused by failure of protein degradation [27,60–63]. Indeed, altered autophagy has been reported in MFM. In skeletal muscle fibers of MFM patients, protein aggregations showed increased expression of

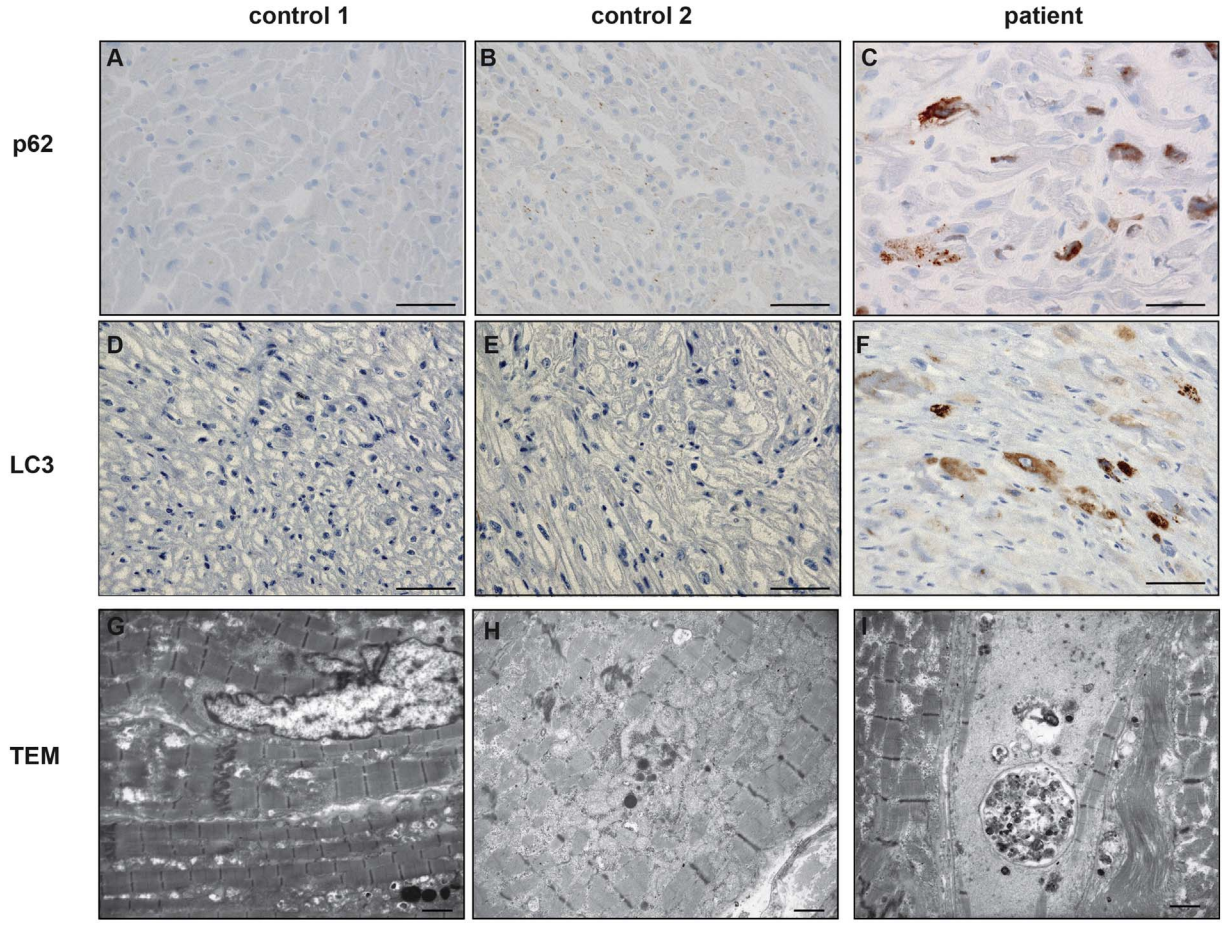

Fig. 5. Morphological analysis of autophagy by immunohistochemistry and TEM. There is no significant expression of p62 and LC3 in the cardiomyocytes of the controls (A, B, D, E), whereas LC3 and p62 positive inclusions are frequent in the patient's cardiomyocytes (C, F). Undegraded autophagosomes, delimited by a double membrane and separated by a cleft, which contain cellular debris, are visible in BAG3-mutant cardiac tissue (I), but not in control samples (G, H). Scale bars: 50 µm (A–F), 2.5 µm (G–I).

proteins involved in proteasomal and autophagic degradation, including BAG3 and ubiquitin [62–64]. In line with this, we detected aggregates expressing BAG3 surrounded by desmin in some cardiomyocytes, as well as an overall increase of the amount of BAG3 and desmin in our patient. These findings are in congruence with studies in a zebrafish model, which have reported an increased aggregation propensity of the BAG3-Pro209Leu mutant protein together with Z-disk proteins such as filamin C [39]. This work has suggested that the BAG3-Pro209Leu mutation leads to a toxic gain of function, by promoting the co-aggregation of mutant and wild-type BAG3, eventually resulting in BAG3 insufficiency and myofibrillar disintegration. Desmin positive aggregates, as seen in our patient's cardiac tissue, have also been described in the skeletal muscle of patients with MFM due to BAG3-Pro209Leu mutation [14,17]. But since desmin upregulation was also described in compensated and decompensated heart failure due to cardiomyopathy [65], we cannot rule out a BAG3-independent desmin upregulation in our patient.

Autophagy is a complex process necessary for removal, recycling and repair of intracellular components. Different types of autophagy exist in muscle, which share common molecular components. Damaged proteins aggregating during contraction (e.g filamin) have to be degraded to maintain Z-disk integrity. BAG3-containing chaperone complexes have been shown to play a crucial role in these removal processes *via* selective macroautophagy. Impairment of BAG3-mediated autophagy has been related to Z-disk disintegration [22,24,27–30,33,34,36].

Autophagy can be analyzed morphologically by electron microscopy, and biochemically by determining the levels of autophagic markers such as p62, LC3 and WIPI by western blotting [46,66]. An important early event in autophagosome formation is the production of phosphatidylinositol 3-phosphate in the membrane of the phagophore. The generated phosphatidylinositol 3-phosphate is bound by proteins of the WIPI family, which are required to promote LC3 lipidation. An increase in WIPI may reflect autophagy induction, but may also result from a blockade of autophagic flux [67]. Microtubule associated protein 1 light chain 3 (LC3) is implicated in macroautophagy and shows two different bands in immunoblotting, the cytosolic form LC3-I and the phosphatidylethanolamine conjugated form LC3-II. An increase of LC3-II, necessary to recruit autophagosomal membranes, indicates an induction of autophagosome formation and subsequent lysosomal fusion and degradation, whereas an increase of LC3-I indicates defective autophagy [68,69]. P62, also known as sequestosome-1 (SQSTM1) or zeta interacting protein (ZIP), is essential for the clearance of ubiquitinated and non-ubiquitinated proteins. It is degraded during autophagy and its level usually inversely correlates with autophagy. Suppression of autophagy leads to accumulation of p62 which further inhibits autophagy by activating MTORC1 [70–74]. In our patient's cardiac tissue, we detected a substantially increased levels of autophagy receptor p62, WIPI1, and LC3-I when compared to control tissues, whereas LC3-II was not altered. Collectively, these findings suggest a defective autophagy in BAG3-Pro209Leu mutated cardiac tissue. In line with this, the total amount of ubiquitinated proteins was higher in the BAG3-mutant tissue than in the control samples, indicating that the marked proteins are not being efficiently degraded.

BAG3 serves as a co-chaperone/nucleotide exchange factor for HSP70 [20] and interacts with proteins of the small heat shock protein

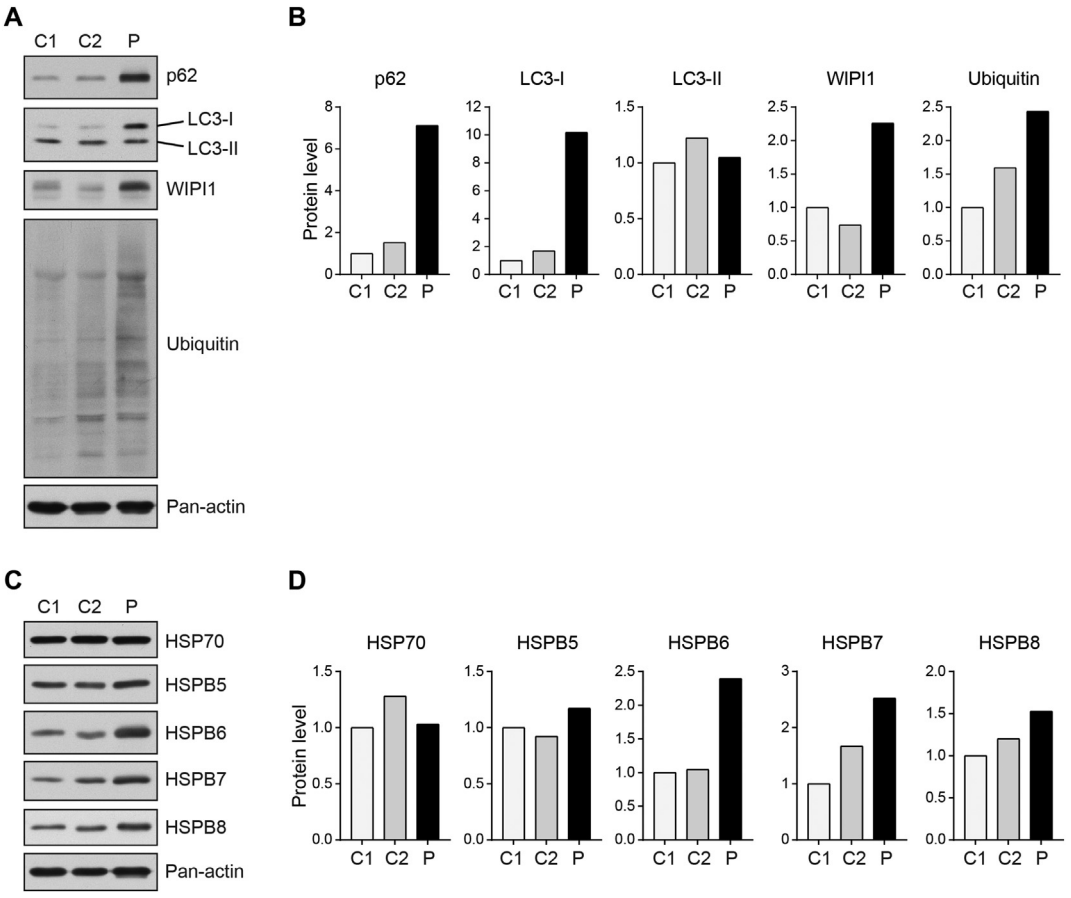

Fig. 6. Western blot analysis of autophagy markers and heat shock proteins in the patient's cardiac muscle (P) compared to control tissue (C1, C2). Equal amounts of total protein were loaded and probed with the indicated antibodies, pan-actin served as a loading control. The autophagic markers p62, LC3-I, WIPI1, as well as the total levels of ubiquitinated proteins are strongly increased in the patient compared to controls, while LC3-II was not altered (A, B). HSP70 expression is not changed in the patient, while small heat shock proteins (HSPB5-8), in particular HSPB6, are upregulated (C, D). The amount of signal was densitometrically quantified and normalized to the level of pan-actin (B, D).

family (HSPBs [47,48]). Moreover, a complex of BAG3 and HSPB8 mediates degradation of mutant and aggregation-prone huntingtin protein by macroautophagy [29]. In addition, BAG3 coordinates the activity of HSP70/HSC70 and HSPB8 for degradation of damaged proteins by selective macroautophagy, which is essential for muscle maintenance in Drosophila [27]. We therefore examined the levels of HSP70 and a set of HSPB proteins in the BAG3-Pro209Leu mutant cardiac tissue. While HSP70 levels were not altered, we found moderate to marked increases of all HSPB proteins tested in the patient's cardiomyocytes. This increment was greatest for HSPB6, which is known to bind BAG3 with high affinity [48]. Interestingly, the Pro209Leu mutation lies within a region of BAG3, which contributes to HSPB protein binding [48], and thus, alters the affinity for HSPBs. This could result in a decreased turnover of HSPBs in cells with mutant BAG3, thereby explaining the elevated levels of these proteins found in our study. Alternatively, compromised binding of BAG3 to HSPBs may induce their accumulation through aggregation. Indeed binding to BAG3 has been shown to promote de-oligomerisation of HSPB1 [48]. This hypothesis is supported by the findings of the present study, demonstrating αB-crystallin (HSPB5) aggregates in the BAG3 mutant cardiac tissue. Furthermore, an altered interaction of BAG3 with HSPBs and/or HSP70 may contribute to the dysregulated autophagy which we observed in our patient.

The role of BAG3 and of the Pro209Leu mutant in the pathogenic mechanism of the skeletal myopathy has been analyzed in several cell culture-based and animal models [18,21,31,39] but the hypothesis that altered autophagy contributes to disease onset has not been tested in human tissue so far. Our data corroborate the notion that the BAG3-Pro209Leu mutation leads to reduced capacity for autophagy of protein aggregates formed during mechanical stress in cardiac muscle [75–78].

Table 2
Mitochondrial enzyme activities in the cardiac muscle of the patient and controls. Enzyme activities are expressed as nmol/min/mg protein. The Z-score shown in brackets is calculated from the logarithm of OXPHOS complex activity divided by the logarithm of the citrate synthase activity. Values lower than − 1.96 are significantly different ($P < 0.05$) from the control samples. Historical control sample ratios are given as mean ± SD.

	Complex I/CS	Complex II/CS	Complex II + III/CS	Complex III/CS	Complex IV/CS	Citrate synthase
Control 1	81 [− 0.13]	78 [− 0.87]	67 [− 0.95]	262 [0.72]	416 [0.73]	627
Control 2	92 [− 0.26]	105 [− 0.51]	109 [− 0.17]	210 [− 0.02]	623 [1.20]	814
Patient	89 [− 0.06]	99 [− 0.34]	114 [0.24]	321 [0.92]	488 [0.94]	691
Controls (historical) (n = 22)	97 ± 28	139 ± 40	126 ± 36	208 ± 33	448 ± 103	869 ± 200

CS = citrate synthase.

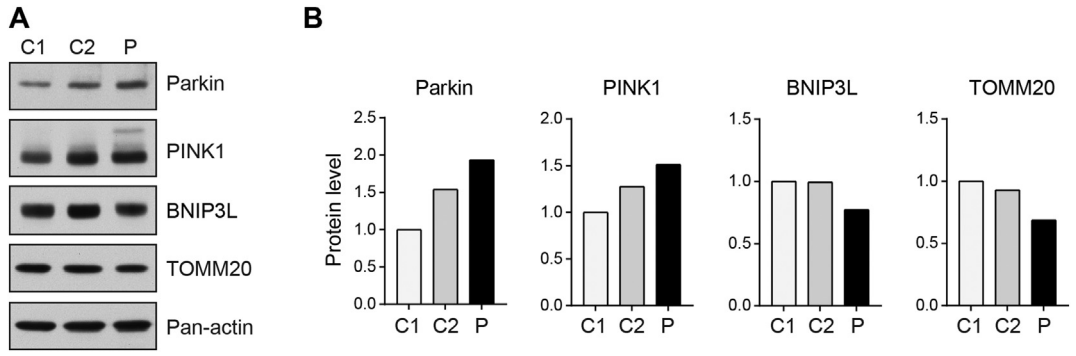

Fig. 7. Western blot analysis of mitochondrial and mitophagy markers in the patient's cardiac tissue (P) compared to control samples (C1, C2). Equal amounts of total protein were loaded and probed with the indicated antibodies, pan-actin served as a loading control (A). The amount of signal was densitometrically quantified and normalized to the level of pan-actin (B).

Therefore, stimulation of autophagy may contribute to enhanced clearance of aggregates [64] and represents a potential therapeutic strategy for RCM in patients with a BAG3-Pro209Leu mutation.

Cardiomyocytes contain large numbers of mitochondria that can become damaged under conditions of cardiac stress. Autophagy of defective mitochondria (mitophagy) is an important mechanism for recycling and rejuvenation of mitochondria [79]. Mitochondrial abnormalities have been described in skeletal muscle biopsy samples from patients with MFM [50,51,80] and recent findings suggest a role of BAG3 in mitochondrial quality control in cardiomyocytes [53]. In our patient's heart explant, we found normal citrate synthase activities and unchanged OXPHOS enzyme activities, indicating that there was no substantial change in mitochodrial number or respiratory function. On the other hand, focal mitochondrial accumulations with enhanced polymorphia and some condensed mitochondria were observed at the ultrastructural level (Fig. 3F). Together with the slight decrease in TOMM20 levels (Fig. 7), these observations are compatible with some degree of mitochondrial impairment. Similarly, the modestly increased expression of parkin and PINK1, which play a critical role in mitophagy by mediating proteasomal degradation of mitochondrial outer membrane proteins [81,82], might be indicative of impairment of mitochondrial function or clearance [53,54], which can be an additional factor in the cardiac pathogenesis elicited by the BAG3-Pro209Leu mutation. In future studies, it will be interesting to assess the involvement of autophagy and mitophagy in the skeletal muscle pathogenesis in patients with BAG3-Pro209Leu mutation.

5. Conclusions

In conclusion, we present the first detailed morphological and biochemical characterization of cardiac tissue in a patient with severe MFM caused by the BAG3-Pro209Leu mutation. BAG3-mutant cardiac tissue showed protein aggregates and myofibrillar disintegration typical for MFM. The morphological alterations were similar, but more severe than those described in skeletal muscle samples, and are consistent with a severe cardiomyopathy. Our results support the hypotheses that dysregulation of autophagy is an important factor contributing to the pathophysiology of RCM in patients with the BAG3-Pro209Leu mutations.

Acknowledgement

The authors thank the patients and their families for their cooperation and permission to publish the data. The authors thank Hannah Schlierbach, Jonas Görlach and Kerstin Leib for their excellent technical assistance.

Conflicts of interest

The authors declare that they have no conflict of interest.

References

[1] N.J. Silvestri, H. Ismail, P. Zimetbaum, E.M. Raynor, Cardiac involvement in the muscular dystrophies, Muscle Nerve (2017), http://dx.doi.org/10.1002/mus.26014.
[2] D. Selcen, Myofibrillar myopathies, Neuromuscul. Disord. 21 (2011) 161–171, http://dx.doi.org/10.1016/j.nmd.2010.12.007.
[3] R. Schroder, B. Schoser, Myofibrillar myopathies: a clinical and myopathological guide, Brain Pathol. 19 (2009) 483–492, http://dx.doi.org/10.1111/j.1750-3639.2009.00289.x.
[4] G. Vattemi, M. Neri, S. Piffer, P. Vicart, F. Gualandi, M. Marini, et al., Clinical, morphological and genetic studies in a cohort of 21 patients with myofibrillar myopathy, Acta Myol. 30 (2011) 121–126.
[5] G. Pfeffer, R. Barresi, I.J. Wilson, S.A. Hardy, H. Griffin, J. Hudson, et al., Titin founder mutation is a common cause of myofibrillar myopathy with early respiratory failure, J. Neurol. Neurosurg. Psychiatry 85 (2014) 331–338, http://dx.doi.org/10.1136/jnnp-2012-304728.
[6] R.A. Kley, M. Olive, R. Schroder, New aspects of myofibrillar myopathies, Curr. Opin. Neurol. 29 (2016) 628–634, http://dx.doi.org/10.1097/wco.0000000000000357.
[7] S. Nakano, A.G. Engel, A.J. Waclawik, A.M. Emslie-Smith, N.A. Busis, Myofibrillar myopathy with abnormal foci of desmin positivity. I. Light and electron microscopy analysis of 10 cases, J. Neuropathol. Exp. Neurol. 55 (1996) 549–562.
[8] M. Olive, Extralysosomal protein degradation in myofibrillar myopathies, Brain Pathol. 19 (2009) 507–515, http://dx.doi.org/10.1111/j.1750-3639.2009.00288.x.
[9] K.G. Claeys, P.F. van der Ven, A. Behin, T. Stojkovic, B. Eymard, O. Dubourg, et al., Differential involvement of sarcomeric proteins in myofibrillar myopathies: a morphological and immunohistochemical study, Acta Neuropathol. 117 (2009) 293–307, http://dx.doi.org/10.1007/s00401-008-0479-7.
[10] F. D'Avila, M. Meregalli, S. Lupoli, M. Barcella, A. Orro, F. De Santis, et al., Exome sequencing identifies variants in two genes encoding the LIM-proteins NRAP and FHL1 in an Italian patient with BAG3 myofibrillar myopathy, J. Muscle Res. Cell Motil. 37 (2016) 101–115, http://dx.doi.org/10.1007/s10974-016-9451-7.
[11] K.G. Claeys, M. Fardeau, R. Schroder, T. Suominen, K. Tolksdorf, A. Behin, et al., Electron microscopy in myofibrillar myopathies reveals clues to the mutated gene, Neuromuscul. Disord. 18 (2008) 656–666, http://dx.doi.org/10.1016/j.nmd.2008.06.367.
[12] C.G. Konersman, B.J. Bordini, G. Scharer, M.W. Lawlor, S. Zangwill, J.F. Southern, et al., BAG3 myofibrillar myopathy presenting with cardiomyopathy, Neuromuscul. Disord. 25 (2015) 418–422, http://dx.doi.org/10.1016/j.nmd.2015.01.009.
[13] D. Selcen, F. Muntoni, B.K. Burton, E. Pegoraro, C. Sewry, A.V. Bite, A.G. Engel, Mutation in BAG3 causes severe dominant childhood muscular dystrophy, Ann. Neurol. 65 (2009) 83–89, http://dx.doi.org/10.1002/ana.21553.
[14] Z. Odgerel, A. Sarkozy, H.S. Lee, C. McKenna, J. Rankin, V. Straub, et al., Inheritance patterns and phenotypic features of myofibrillar myopathy associated with a BAG3 mutation, Neuromuscul. Disord. 20 (2010) 438–442, http://dx.doi.org/10.1016/j.nmd.2010.05.004.
[15] A. Kostera-Pruszczyk, M. Suszek, R. Ploski, M. Franaszczyk, A. Potulska-Chromik, P. Pruszczyk, et al., BAG3-related myopathy, polyneuropathy and cardiomyopathy with long QT syndrome, J. Muscle Res. Cell Motil. 36 (2015) 423–432, http://dx.doi.org/10.1007/s10974-015-9431-3.
[16] H.C. Lee, S.W. Cherk, S.K. Chan, S. Wong, T.W. Tong, W.S. Ho, et al., BAG3-related myofibrillar myopathy in a Chinese family, Clin. Genet. 81 (2012) 394–398, http://dx.doi.org/10.1111/j.1399-0004.2011.01659.x.
[17] F. Jaffer, S.M. Murphy, M. Scoto, E. Healy, A.M. Rossor, S. Brandner, et al., BAG3 mutations: another cause of giant axonal neuropathy, J. Peripher. Nerv. Syst. 17 (2012) 210–216, http://dx.doi.org/10.1111/j.1529-8027.2012.00409.x.
[18] S. Homma, M. Iwasaki, G.D. Shelton, E. Engvall, J.C. Reed, S. Takayama, BAG3 deficiency results in fulminant myopathy and early lethality, Am. J. Pathol. 169 (2006) 761–773, http://dx.doi.org/10.2353/ajpath.2006.060250.
[19] A. Rosati, V. Graziano, V. De Laurenzi, M. Pascale, M.C. Turco, BAG3: a multifaceted protein that regulates major cell pathways, Cell Death Dis. 2 (2011) e141, , http://dx.doi.org/10.1038/cddis.2011.24.
[20] C. Behl, Breaking BAG: the co-chaperone BAG3 in health and disease, Trends

Pharmacol. Sci. 37 (2016) 672–688, http://dx.doi.org/10.1016/j.tips.2016.04.007.
[21] L.M. Judge, J.A. Perez-Bermejo, A. Truong, A.J. Ribeiro, J.C. Yoo, C.L. Jensen, et al., A BAG3 chaperone complex maintains cardiomyocyte function during proteotoxic stress, JCI Insight 2 (2017), http://dx.doi.org/10.1172/jci.insight.94623.
[22] C. Klimek, B. Kathage, J. Wordehoff, J. Hohfeld, BAG3-mediated proteostasis at a glance, J. Cell Sci. 130 (2017) 2781–2788, http://dx.doi.org/10.1242/jcs.203679.
[23] M. Gamerdinger, S. Carra, C. Behl, Emerging roles of molecular chaperones and co-chaperones in selective autophagy: focus on BAG proteins, J. Mol. Med. (Berl.) 89 (2011) 1175–1182, http://dx.doi.org/10.1007/s00109-011-0795-6.
[24] M. Gamerdinger, A.M. Kaya, U. Wolfrum, A.M. Clement, C. Behl, BAG3 mediates chaperone-based aggresome-targeting and selective autophagy of misfolded proteins, EMBO Rep. 12 (2011) 149–156, http://dx.doi.org/10.1038/embor.2010.203.
[25] T. Cullup, A.L. Kho, C. Dionisi-Vici, B. Brandmeier, F. Smith, Z. Urry, et al., Recessive mutations in EPG5 cause vici syndrome, a multisystem disorder with defective autophagy, Nat. Genet. 45 (2013) 83–87, http://dx.doi.org/10.1038/ng.2497.
[26] M. Ganassi, D. Mateju, I. Bigi, L. Mediani, I. Poser, H.O. Lee, et al., A surveillance function of the HSPB8-BAG3-HSP70 chaperone complex ensures stress granule integrity and dynamism, Mol. Cell 63 (2016) 796–810, http://dx.doi.org/10.1016/j.molcel.2016.07.021.
[27] V. Arndt, N. Dick, R. Tawo, M. Dreiseidler, D. Wenzel, M. Hesse, et al., Chaperone-assisted selective autophagy is essential for muscle maintenance, Curr. Biol. 20 (2010) 143–148, http://dx.doi.org/10.1016/j.cub.2009.11.022.
[28] S. Carra, S.J. Seguin, H. Lambert, J. Landry, HspB8 chaperone activity toward poly (Q)-containing proteins depends on its association with Bag3, a stimulator of macroautophagy, J. Biol. Chem. 283 (2008) 1437–1444, http://dx.doi.org/10.1074/jbc.M706304200.
[29] S. Carra, S.J. Seguin, J. Landry, HspB8 and Bag3: a new chaperone complex targeting misfolded proteins to macroautophagy, Autophagy 4 (2008) 237–239.
[30] M. Gamerdinger, P. Hajieva, A.M. Kaya, U. Wolfrum, F.U. Hartl, C. Behl, Protein quality control during aging involves recruitment of the macroautophagy pathway by BAG3, EMBO J. 28 (2009) 889–901, http://dx.doi.org/10.1038/emboj.2009.29.
[31] A. Hishiya, T. Kitazawa, S. Takayama, BAG3 and Hsc70 interact with actin capping protein CapZ to maintain myofibrillar integrity under mechanical stress, Circ. Res. 107 (2010) 1220–1231, http://dx.doi.org/10.1161/circresaha.110.225649.
[32] M. Minoia, A. Boncoraglio, J. Vinet, F.F. Morelli, J.F. Brunsting, A. Poletti, et al., BAG3 induces the sequestration of proteasomal clients into cytoplasmic puncta: implications for a proteasome-to-autophagy switch, Autophagy 10 (2014) 1603–1621, http://dx.doi.org/10.4161/auto.29409.
[33] A. Ulbricht, F.J. Eppler, V.E. Tapia, P.F. van der Ven, N. Hampe, N. Hersch, et al., Cellular mechanotransduction relies on tension-induced and chaperone-assisted autophagy, Curr. Biol. 23 (2013) 430–435, http://dx.doi.org/10.1016/j.cub.2013.01.064.
[34] A. Ulbricht, S. Gehlert, B. Leciejewski, T. Schiffer, W. Bloch, J. Hohfeld, Induction and adaptation of chaperone-assisted selective autophagy CASA in response to resistance exercise in human skeletal muscle, Autophagy 11 (2015) 538–546, http://dx.doi.org/10.1080/15548627.2015.1017186.
[35] A. Ulbricht, J. Hohfeld, Tension-induced autophagy: may the chaperone be with you, Autophagy 9 (2013) 920–922, http://dx.doi.org/10.4161/auto.24213.
[36] B. Kathage, S. Gehlert, A. Ulbricht, L. Ludecke, V.E. Tapia, Z. Orfanos, et al., The cochaperone BAG3 coordinates protein synthesis and autophagy under mechanical strain through spatial regulation of mTORC1, Biochim. Biophys. Acta 1864 (2017) 62–75, http://dx.doi.org/10.1016/j.bbamcr.2016.10.007.
[37] N. Norton, D. Li, M.J. Rieder, J.D. Siegfried, E. Rampersaud, S. Zuchner, et al., Genome-wide studies of copy number variation and exome sequencing identify rare variants in BAG3 as a cause of dilated cardiomyopathy, Am. J. Hum. Genet. 88 (2011) 273–282, http://dx.doi.org/10.1016/j.ajhg.2011.01.016.
[38] D.Y. Youn, D.H. Lee, M.H. Lim, J.S. Yoon, J.H. Lim, S.E. Jung, et al., Bis deficiency results in early lethality with metabolic deterioration and involution of spleen and thymus, Am. J. Physiol. Endocrinol. Metab. 295 (2008) E1349–E1357, http://dx.doi.org/10.1152/ajpendo.90704.2008.
[39] A.A. Ruparelia, V. Oorschot, R. Vaz, G. Ramm, R.J. Bryson-Richardson, Zebrafish models of BAG3 myofibrillar myopathy suggest a toxic gain of function leading to BAG3 insufficiency, Acta Neuropathol. 128 (2014) 821–833, http://dx.doi.org/10.1007/s00401-014-1344-5.
[40] J.B. Noury, T. Maisonobe, P. Richard, V. Delague, E. Malfatti, T. Stojkovic, Rigid spine syndrome associated with sensory-motor axonal neuropathy resembling Charcot-Marie-tooth disease is characteristic of Bcl-2-associated athanogene-3 gene mutations even without cardiac involvement, Muscle Nerve (2017), http://dx.doi.org/10.1002/mus.25631.
[41] M.F. Dohrn, N. Glockle, L. Mulahasanovic, C. Heller, J. Mohr, C. Bauer, et al., Frequent genes in rare diseases: panel-based next generation sequencing to disclose causal mutations in hereditary neuropathies, J. Neurochem. (2017), http://dx.doi.org/10.1111/jnc.14217.
[42] J. Schindelin, I. Arganda-Carreras, E. Frise, V. Kaynig, M. Longair, T. Pietzsch, et al., Fiji: an open-source platform for biological-image analysis, Nat. Methods 9 (2012) 676–682, http://dx.doi.org/10.1038/nmeth.2019.
[43] Y. Hatefi, D.L. Stiggall, Preparation and properties of succinate: ubiquinone oxidoreductase (complex II), Methods Enzymol. 53 (1978) 21–27.
[44] P. Rustin, D. Chretien, T. Bourgeron, B. Gerard, A. Rotig, J.M. Saudubray, A. Munnich, Biochemical and molecular investigations in respiratory chain deficiencies, Clin. Chim. Acta 228 (1994) 35–51.
[45] S. DiMauro, S. Servidei, M. Zeviani, M. DiRocco, D.C. DeVivo, S. DiDonato, et al., Cytochrome c oxidase deficiency in Leigh syndrome, Ann. Neurol. 22 (1987) 498–506, http://dx.doi.org/10.1002/ana.410220409.
[46] E.L. Eskelinen, A.L. Kovacs, Double membranes vs. lipid bilayers, and their significance for correct identification of macroautophagic structures, Autophagy 7 (2011) 931–932.
[47] M. Fuchs, D.J. Poirier, S.J. Seguin, H. Lambert, S. Carra, S.J. Charette, J. Landry, Identification of the key structural motifs involved in HspB8/HspB6-Bag3 interaction, Biochem. J. 425 (2009) 245–255, http://dx.doi.org/10.1042/BJ20090907.
[48] J.N. Rauch, E. Tse, R. Freilich, S.A. Mok, L.N. Makley, D.R. Southworth, J.E. Gestwicki, BAG3 is a modular, scaffolding protein that physically links heat shock protein 70 (Hsp70) to the small heat shock proteins, J. Mol. Biol. 429 (2017) 128–141, http://dx.doi.org/10.1016/j.jmb.2016.11.013.
[49] A.E. Vincent, J.P. Grady, M.C. Rocha, C.L. Alston, K.A. Rygiel, R. Barresi, et al., Mitochondrial dysfunction in myofibrillar myopathy, Neuromuscul. Disord. 26 (2016) 691–701, http://dx.doi.org/10.1016/j.nmd.2016.08.004.
[50] S. Jackson, J. Schaefer, M. Meinhardt, H. Reichmann, Mitochondrial abnormalities in the myofibrillar myopathies, Eur. J. Neurol. 22 (2015) 1429–1435, http://dx.doi.org/10.1111/ene.12814.
[51] P.R. Joshi, A. Hauburger, R. Kley, K.G. Claeys, I. Schneider, W. Kress, et al., Mitochondrial abnormalities in myofibrillar myopathies, Clin. Neuropathol. 33 (2014) 134–142, http://dx.doi.org/10.5414/np300693.
[52] M. Iglewski, J.A. Hill, S. Lavandero, B.A. Rothermel, Mitochondrial fission and autophagy in the normal and diseased heart, Curr. Hypertens. Rep. 12 (2010) 418–425, http://dx.doi.org/10.1007/s11906-010-0147-x.
[53] F.G. Tahrir, T. Knezevic, M.K. Gupta, J. Gordon, J.Y. Cheung, A.M. Feldman, K. Khalili, Evidence for the role of BAG3 in mitochondrial quality control in cardiomyocytes, J. Cell. Physiol. 232 (2017) 797–805, http://dx.doi.org/10.1002/jcp.25476.
[54] D. Narendra, A. Tanaka, D.F. Suen, R.J. Youle, Parkin is recruited selectively to impaired mitochondria and promotes their autophagy, J. Cell Biol. 183 (2008) 795–803, http://dx.doi.org/10.1083/jcb.200809125.
[55] C. Kang, M.A. Badr, V. Kyrychenko, E.L. Eskelinen, N. Shirokova, Deficit in PINK1-PARKIN mediated mitochondrial autophagy at late stages of dystrophic cardiomyopathy, Cardiovasc. Res. (2017), http://dx.doi.org/10.1093/cvr/cvx201.
[56] M. Lazarou, D.A. Sliter, L.A. Kane, S.A. Sarraf, C. Wang, J.L. Burman, et al., The ubiquitin kinase PINK1 recruits autophagy receptors to induce mitophagy, Nature 524 (2015) 309–314, http://dx.doi.org/10.1038/nature14893.
[57] I. Novak, Mitophagy: a complex mechanism of mitochondrial removal, Antioxid. Redox Signal. 17 (2012) 794–802, http://dx.doi.org/10.1089/ars.2011.4407.
[58] R.Y. Shi, S.H. Zhu, V. Li, S.B. Gibson, X.S. Xu, J.M. Kong, BNIP3 interacting with LC3 triggers excessive mitophagy in delayed neuronal death in stroke, CNS Neurosci. Ther. 20 (2014) 1045–1055, http://dx.doi.org/10.1111/cns.12325.
[59] M. Olive, L.G. Goldfarb, A. Shatunov, D. Fischer, I. Ferrer, Myotilinopathy: refining the clinical and myopathological phenotype, Brain 128 (2005) 2315–2326, http://dx.doi.org/10.1093/brain/awh576.
[60] J.L. De Bleecker, A.G. Engel, B.B. Ertl, Myofibrillar myopathy with abnormal foci of desmin positivity. II. Immunocytochemical analysis reveals accumulation of multiple other proteins, J. Neuropathol. Exp. Neurol. 55 (1996) 563–577.
[61] M. Olive, Z. Odgerel, A. Martinez, J.J. Poza, F.G. Bragado, R.J. Zabalza, et al., Clinical and myopathological evaluation of early- and late-onset subtypes of myofibrillar myopathy, Neuromuscul. Disord. 21 (2011) 533–542, http://dx.doi.org/10.1016/j.nmd.2011.05.002.
[62] R.A. Kley, P. Serdaroglu-Oflazer, Y. Leber, Z. Odgerel, P.F. van der Ven, M. Olive, et al., Pathophysiology of protein aggregation and extended phenotyping in filaminopathy, Brain 135 (2012) 2642–2660, http://dx.doi.org/10.1093/brain/aws200.
[63] R.A. Kley, P.F. van der Ven, M. Olive, J. Hohfeld, L.G. Goldfarb, D.O. Furst, M. Vorgerd, Impairment of protein degradation in myofibrillar myopathy caused by FLNC/filamin C mutations, Autophagy 9 (2013) 422–423, http://dx.doi.org/10.4161/auto.22921.
[64] A.A. Ruparelia, V. Oorschot, G. Ramm, R.J. Bryson-Richardson, FLNC myofibrillar myopathy results from impaired autophagy and protein insufficiency, Hum. Mol. Genet. 25 (2016) 2131–2142, http://dx.doi.org/10.1093/hmg/ddw080.
[65] A. Gupta, S. Gupta, D. Young, B. Das, J. McMahon, S. Sen, Impairment of ultrastructure and cytoskeleton during progression of cardiac hypertrophy to heart failure, Lab. Investig. 90 (2010) 520–530, http://dx.doi.org/10.1038/labinvest.2010.43.
[66] D.J. Klionsky, K. Abdelmohsen, A. Abe, M.J. Abedin, H. Abeliovich, A. Acevedo Arozena, et al., Guidelines for the use and interpretation of assays for monitoring autophagy (3rd edition), Autophagy 12 (2016) 1–222, http://dx.doi.org/10.1080/15548627.2015.1100356.
[67] T. Proikas-Cezanne, Z. Takacs, P. Donnes, O. Kohlbacher, WIPI proteins: essential PtdIns3P effectors at the nascent autophagosome, J. Cell Sci. 128 (2015) 207–217, http://dx.doi.org/10.1242/jcs.146258.
[68] N. Mizushima, T. Yoshimori, How to interpret LC3 immunoblotting, Autophagy 3 (2007) 542–545.
[69] I. Tanida, T. Ueno, E. Kominami, LC3 and autophagy, Methods Mol. Biol. 445 (2008) 77–88, http://dx.doi.org/10.1007/978-1-59745-157-4_4.
[70] A. Duran, R. Amanchy, J.F. Linares, J. Joshi, S. Abu-Baker, A. Porollo, et al., p62 is a key regulator of nutrient sensing in the mTORC1 pathway, Mol. Cell 44 (2011) 134–146, http://dx.doi.org/10.1016/j.molcel.2011.06.038.
[71] S. Manley, J.A. Williams, W.X. Ding, Role of p62/SQSTM1 in liver physiology and pathogenesis, Exp. Biol. Med. (Maywood) 238 (2013) 525–538, http://dx.doi.org/10.1177/1535370213489446.
[72] T. Johansen, T. Lamark, Selective autophagy mediated by autophagic adapter proteins, Autophagy 7 (2011) 279–296.
[73] C. Kraft, M. Peter, K. Hofmann, Selective autophagy: ubiquitin-mediated recognition and beyond, Nat. Cell Biol. 12 (2010) 836–841, http://dx.doi.org/10.1038/ncb0910-836.

[74] M. Lippai, P. Low, The role of the selective adaptor p62 and ubiquitin-like proteins in autophagy, Biomed. Res. Int. 2014 (2014) 832704, http://dx.doi.org/10.1155/2014/832704.
[75] T. Knezevic, V.D. Myers, J. Gordon, D.G. Tilley, T.E. Sharp, J. Wang 3rd, et al., BAG3: a new player in the heart failure paradigm, Heart Fail. Rev. 20 (2015) 423–434, http://dx.doi.org/10.1007/s10741-015-9487-6.
[76] J. Zhang, Z. He, W. Xiao, Q. Na, T. Wu, K. Su, X. Cui, Overexpression of BAG3 attenuates hypoxia-induced cardiomyocyte apoptosis by inducing autophagy, Cell. Physiol. Biochem. 39 (2016) 491–500, http://dx.doi.org/10.1159/000445641.
[77] P. Tannous, H. Zhu, A. Nemchenko, J.M. Berry, J.L. Johnstone, J.M. Shelton, et al., Intracellular protein aggregation is a proximal trigger of cardiomyocyte autophagy, Circulation 117 (2008) 3070–3078, http://dx.doi.org/10.1161/circulationaha.107.763870.
[78] T. Arimura, T. Ishikawa, S. Nunoda, S. Kawai, A. Kimura, Dilated cardiomyopathy-associated BAG3 mutations impair Z-disc assembly and enhance sensitivity to apoptosis in cardiomyocytes, Hum. Mutat. 32 (2011) 1481–1491, http://dx.doi.org/10.1002/humu.21603.
[79] V. Parra, H. Verdejo, A. del Campo, C. Pennanen, J. Kuzmicic, M. Iglewski, et al., The complex interplay between mitochondrial dynamics and cardiac metabolism, J. Bioenerg. Biomembr. 43 (2011) 47–51, http://dx.doi.org/10.1007/s10863-011-9332-0.
[80] J. Reimann, W.S. Kunz, S. Vielhaber, K. Kappes-Horn, R. Schroder, Mitochondrial dysfunction in myofibrillar myopathy, Neuropathol. Appl. Neurobiol. 29 (2003) 45–51.
[81] S. Geisler, K.M. Holmstrom, D. Skujat, F.C. Fiesel, O.C. Rothfuss, P.J. Kahle, W. Springer, PINK1/Parkin-mediated mitophagy is dependent on VDAC1 and p62/SQSTM1, Nat. Cell Biol. 12 (2010) 119–131, http://dx.doi.org/10.1038/ncb2012.
[82] P. Wild, I. Dikic, Mitochondria get a Parkin' ticket, Nat. Cell Biol. 12 (2010) 104–106, http://dx.doi.org/10.1038/ncb0210-104.